

Competitive Hydrogen-Bonding Interactions in Modified Polymer Membranes: A Density Functional Theory Investigation

G. De Luca,^{*,†} A. Gugliuzza,[†] and E. Drioli^{†,‡}

Research Institute on Membrane Technology (ITM-CNR) and Department of Chemical Engineering and Materials, University of Calabria, Via P. Bucci, I-87030 Rende (CS), Italy

Received: January 9, 2009; Revised Manuscript Received: February 25, 2009

The subject of this work is the density functional theory (DFT) investigation of competitive hydrogen-bonding interactions that occur in modified block poly(ether/amide) (PEBAX) membranes. Previously, an evaluation of hydrogen-bonding interactions occurring between *N*-ethyl-*o,p*-toluensulfonamide (KET) modifiers was performed to establish the role of these interactions in affinity processes when the modifier is dissolved in PEBAX matrixes. However, some issues related to polymer–polymer (host–host) and modifier–polymer (host–guest) interactions were not analyzed from a theoretical point of view in the previous analysis. Here, a comparative computational analysis of these intermolecular interactions is discussed. New insights into the role of hydrogen bonding in domino processes are provided. Calculations in solvent and in vacuum have been done, yielding indications about the change in the availability of the polar groups of the polymer, which is considered to be partially responsible for the enhanced hydrophilicity of the membranes. This study can open the way to the construction of new predictive quantum modeling approaches for designing improved modifiers, enabling the optimization of polymer membrane performance.

Introduction

The chemical modification of polymer membranes is a powerful tool for regulating the transport properties through films largely used in the food and beverage packaging,¹ pharmaceutical,^{2,3} textile,^{4,5} and gas separation industries.^{6–8} Plasmas, polymer blends, and addition of low-molecular-weight modifiers represent some of the many approaches used for changing the physicochemical properties of these membranes. Mostly, modifiers inside polymer matrixes are an attractive strategy for changing local chemical environments and, thereby, controlling the penetration of molecules into the polymer matrixes and regulating intra- and intermolecular interactions.^{9–11} The controlling structure–property relationships, therefore, appear to be of crucial importance in selecting suitable modifiers (guests) for enhancing the performance of the membranes (hosts). With this concern, macroscopic modifications in the transport properties can often be attributed to simple intermolecular interactions such as hydrogen bonding, occurring between modifier and modifier, between polymer and modifier, and between polymer and polymer. Within this framework, hydrogen bonding represents the interaction for excellence and can often be responsible for dramatic domino effects. For example, when a modifier is dissolved in a polymer matrix having chemical groups that interact noncovalently with it, polymer–polymer interactions are broken, and new polymer–modifier bonds are formed. This effect can change intrinsic polymer properties such as hydrophilicity/hydrophobicity or the packing density of the polymer chains.

This type of interaction effectively plays a crucial role, for example, in the adsorption of polar and quadrupolar molecules, as when *N*-ethyl-*o,p*-toluensulfonamide (KET) is blended with

block poly(ether/amide) (PEBAX) materials.^{6,8,9,12} No linear sorption of these penetrants was experimentally observed in PEBAX matrixes, as the KET content rose. Experimental evidence indicates that both a change in the chemical affinity and structural modifications of the membranes occur. Surface energy modifications and gradual reduction of the packing density of the polymer chains have been extensively investigated.^{9,12} Concerning this change in the membrane chemical affinity, previous theoretical studies provided interesting indications about the influence of guest–guest interactions on the water sorption into modified block poly(ether/amide) membranes.^{13,14} In particular, KET clusters were shown to have less affinity with water than single modifier (i.e., KET) molecules. The constraint of the polymer chains embedding the modifier were further thought to play a crucial role in the affinity properties of the KET clusters, although competitive polymer–polymer (host–host) and polymer–modifier (guest–host) interactions were not examined. Thus, the subject of this work is an extensive density functional theory (DFT) investigation of the influence of intramolecular and intermolecular interactions occurring both among the polar moieties of the polymer and between the sulfonamide linkage and the same polymer groups. In other words, host–host (amide–amide and amide–ester) and guest–host (KET–amide and KET–ester) interactions have been analyzed. These interactions were examined in vacuum and in solvent in order to simulate what usually occurs during membrane fabrication. Experimentally, casting solutions have been prepared from polymer and modifier homogeneously mixed in a solvent. Then, the polymer dopes are cast on glass supports, and the solvent is completely evaporated, leaving dense polymer membranes.

The main focus of this in-depth theoretical study is, therefore, the analysis of crucial hydrogen bonding in domino processes, enabling regulation of the level of sorption of polar and/or polarizable molecules in modified PEBAX membranes. An effect of competitive hydrogen-bonding interactions should be

* Corresponding author. Tel.: +39 (0984) 492027. Fax: +39 (0984) 402103. E-mail: g.deluca@itm.cnr.it. Homepage: www.itm.cnr.it.

[†] Research Institute on Membrane Technology (ITM-CNR).

[‡] Department of Chemical Engineering and Materials.

an increased availability of polymer polar moieties and a correlated decline of the membrane packing density, when KET is dissolved with PEBAX.

The analysis of hydrogen bonding in competitive interaction processes appears to be of crucial importance for the interpretation of phenomena at macroscopic length scales. Hence, this study provides useful indications about some behaviors frequently observed in nature.

Computational Details

The results presented in this work were carried out using the NWChem software package¹⁵ within the framework of density functional theory. Hybrid potentials and energy functionals, namely, the Becke–Lee–Yang–Parr¹⁶ (B3LYP) and X3LYP,^{15,17} were used to take into account the exchange and correlation of electrons. The calculations were performed using linear combinations of Gaussian-type orbitals, whereas Coulomb and exchange-correlation potentials were numerically integrated on an adaptive grid with medium accuracy.¹⁵ Double- ζ orbital bases for C, O, N, H, and S with a polarization function (6-31G*) were employed in conjunction with the B3LYP functional, whereas a triple- ζ orbital basis set (6-311G**) was considered for X3LYP calculations. The energy convergence threshold was set to 10^{-6} au for the self-consistent field procedure, and the root-mean square of the electron density was set to 10^{-5} au. No level shifting was used to obtain convergence of the self-consistent field energy, whereas the DIIS (direct inversion of iterative subspace) option was used. Recently, van der Wijst et al.¹⁸ compared the hydrogen-bond distances and bond energies obtained using nine DFT functionals for adenine–thymine and guanine–cytosine pairs with the results of *ab initio* second-order Møller–Plesset perturbation theory and coupled-cluster calculations. For the systems considered, the calculations of van der Wijst et al. showed that the Becke–Perdew 86 functional better reproduces the bond energies than does the B3LYP functional; indeed, the latter functional overestimates the bond energies by 0.6 kcal/mol for the adenine–thymine pair and by 0.4 kcal/mol for the guanine–cytosine pair. Here, the X3LYP functional optimized for hydrogen bonds¹⁷ has been used; therefore, a comparison between the two hybrid functionals would also be interesting, although this is not the specific objective of this work.

All molecular structures were fully optimized using analytical energy gradients and the quasi-Newton optimization with approximate energy Hessian updates.¹⁵ The optimization convergence was based on the maximum and root-mean-square gradient thresholds of 1.5×10^{-5} and 1.0×10^{-5} , respectively, in conjunction with the maximum and root-mean square of the Cartesian displacement vectors with thresholds of 6.0×10^{-5} and 4.0×10^{-5} , respectively.

From a theoretical point of view, the DFT study of hydrogen bonding should be considered an open and relevant issue. Although calculations of intermolecular energies using some functionals are not very accurate, increasing numbers of hybrid functionals such as X3LYP are used to describe hydrogen bonds. These hybrid functionals have yielded reasonable results in the study of long-range and hydrogen interactions.^{19–23} Extended quantitative studies of covalent and noncovalent hydrogen bonding have defined optimized $\text{N}\cdots\text{H}\cdots\text{O}$ bond lengths of <2 Å as the conventional hydrogen-bonding interaction.^{24–27} This rather unrefined criterion has been used to classify intermolecular interactions in agreement with previous statement. Thus, the distance between the two parts of the bond (e.g., O and H) has to be less than 2 Å for the interaction to be

accepted as hydrogen bonding, without the need of further characterizations.^{21,28–33} However, it is obvious that the policy to take into account the internuclear separation between the donor and acceptor is not sufficient to establish the presence of a hydrogen bond. Hence, an accurate analysis of the electron density described by the wave function of the considered models would be necessary. However, the purpose of this article is to compare the interaction energies of all possible host–host and guest–host adducts in a modified polymer membrane and not to characterize the single interactions. For this reason, the term hydrogen bonding will be used exclusively to indicate a particular configuration of atoms ($\text{X}\cdots\text{H}\cdots\text{Y}$) with internuclear separations of less than 2 Å.

Two approaches are generally used to treat solute–solvent interactions using quantum mechanics: continuum methods and discrete methods. In continuum methods, the solvent is considered as a continuum having a uniform dielectric constant and surrounding the solute molecule placed in a cavity.^{34,35} In this respect, the effect of the solvent is taken into account through a self-consistent reaction field caused by the electrical field of each solute molecule. This reaction field takes into account the polarization of the solvent molecules. The polarization effect of the solvent is evaluated by using a response function, depending on the macroscopic dielectric constant of the solvent and the shape of the cavity.^{34,35} The various continuum methods differ in the ways in which the cavity and the self-consistent reaction field are defined.³⁵ In contrast, in discrete models, the solvent molecules are explicitly considered by means of solvent–solute clusters (supermolecules). In this case, the effect of the solvent is considered in the minimum-energy conformation of the supermolecule. However, when the number of possible cluster configurations is high, this quantum mechanics procedure is computationally very expensive. The solvent–solute configurations can, therefore, be calculated at nonzero Kelvin temperatures using Monte Carlo or molecular dynamics simulations.³⁶

Keeping in mind the types of interactions to be analyzed here, the use of a continuum model represents a good compromise between accuracy and computational costs. In this work, the continuum conductor-like screening model (COSMO), proposed by Klamt and Schüürmann,³⁷ was used. The cavity in which the solute molecule is located is defined as interlocking atomic spheres constructed using specific atomic radii. The radius associated with each atom of solute, along with the corresponding molecule-shaped cavity, is a critical and adjustable parameter in the framework of continuum methods. Different procedures for the estimation of this radius have been proposed.^{38–40} However, this issue goes beyond the scope of this article. The default radii implemented in the NWChem package were used here. The use of these radii justifies the utilization of an “accessibility solvent parameter” equal to 0.^{35,37} Finally, the dielectric constant used here was set equal to 19.9.

The intermolecular interaction energies were evaluated. Specifically, the difference between the energy of an adduct and the sum of the energies of the single components was determined. In addition, the basis set superposition error was also included in the interaction energies according to the counterpoise method.⁴¹

Results and Discussion

Previously, water sorption in modified block poly(ether/amide) membranes was accurately examined by analyzing the influence of hydrogen-bonding interactions between guest and guest. In a continuation of this previous work,¹⁴ here, a comparative investigation of host–host and host–guest interactions as controlling factors for the sorption processes of polar

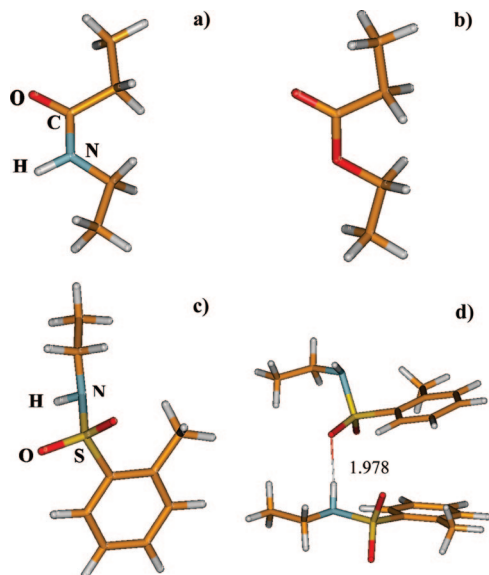


Figure 1. Modeling molecules representative of the functional linkage of PEBAX and modifier structure: (a) amide and (b) ester functional groups, (c) KET modifier, and (d) dimer of KET.

TABLE 1: Intermolecular Interaction Energies in the Solvent at the B3LYP/6-31G* and X3LYP/6-311G Levels of Theory**

system	ΔE_{int} (kcal/mol)	$ \Delta E^{\text{H-H}}_{\text{int}} / \Delta E^{\text{G-H}}_{\text{int}} $
(a) B3LYP/6-31G*		
amide–amide	−4.30	
KET–amide	−2.88	1.5
ester–amide	0.36	
KET–ester	0.18	2.0
KET–KET	0.70	6.1 ^a
(b) X3LYP/6-311G**		
amide–amide	−3.73	
KET–amide	−3.39	1.1
ester–amide	0.56	
KET–ester	−0.18	3.1

^a Amide–amide interaction energy on KET–KET energy.

molecules in membranes has been performed. Polar functional groups of PEBAX enabling the formation of hydrogen bonds have been considered, and all possible combinations have been examined: amide–amide, ester–amide, KET–amide, and KET–ester. To achieve an extensive quantum treatment of all hydrogen bonds involved in the system, modeling molecules have been constructed as representative of the functional linkage in PEBAX. The related structures were optimized and are reported in Figure 1.

The computational strategy was selected according to the experimental methodology used for the fabrication of the membranes: PEBAX and KET were blended at different stoichiometric ratios and dissolved at 80 °C in a mixture of solvents with almost equal dielectric constants. When the temperature was increased, the clear and homogeneous polymer dopes were cast on glass supports, and the solvents were completely evaporated.

The intermolecular interaction energies in solvent were calculated according to the levels of theory previously described. The values are reported in Table 1. The ratios between the absolute values of these energies appear to be completely comparable for the amide–amide and KET–amide adducts (Table 1). The interaction between the modifier and amide group of PEBAX is competitive with that between two amide groups

TABLE 2: Intermolecular Interaction Energies in Vacuum at the B3LYP/6-31G* and X3LYP/6-311G Levels of Theory**

system	ΔE_{int} (kcal/mol)	$ \Delta E^{\text{H-H}}_{\text{int}} / \Delta E^{\text{G-H}}_{\text{int}} $	figure
(a) B3LYP/6-31G*			
amide–amide	−13.19		Figure 2 a
KET–amide	−11.83	1.11	Figure 3 a
ester–amide	−5.43		Figure 2c
KET–ester	−5.65	0.96	Figure 3d
KET–KET ^a	−12.20	1.08	Figure 1d
(b) X3LYP/6-311G**			
amide–amide	−13.77		
KET–amide	−12.84	1.07	
ester–amide	−6.41		
KET–ester	−7.24	0.89	

^a From ref 14.

in the polymer. Both of these interactions were found to be stronger than those between the pairs ester–amide and KET–ester (Table 1). This would imply that amide–amide and KET–amide adducts are more likely to form in solvent than the other adducts. Moreover, from Table 1, it appears that the ester group preferentially interacts with KET compared to the amide group of the polymer. These results suggest that interactions among amide groups and ester–amide coupling are partially prevented at low concentrations of KET in the casting solution. As a consequence, a reduction of the polymer packing density would take place after solvent evaporation, as the experimental analysis highlighted.⁹ Hence, the reduction of the polymer packing density promotes higher availability of the polar groups of the matrix, leading to enhanced membrane hydrophilicity.^{9,10} This interpretation was corroborated by the results obtained in vacuum, that is, when all of the solvent molecules had completely evaporated.

The interaction energies calculated in the absence of solvent are reported in Table 2. First, all energies referred to the adducts involving the ester group exhibit negative values, in contrast to the what was evaluated in the solvent, with the exception of the interaction between KET and ester calculated at the X3LYP level. The evaporation of solvent molecules stabilizes the adducts involving ester groups, even though the amide–amide and KET–amide interactions appear to be even stronger than those between ester–amide and KET–ester moieties. Nevertheless, the ratios of the absolute values of the interaction energies confirm in vacuum what was observed in solvent. Despite the weakness of the KET–KET interaction in solvent (Table 1), in vacuum, the modifier–modifier interaction was found to be more competitive than the amide–amide interaction (Table 2). This suggests that the KET–KET adduct could affect the water sorption at higher concentration of modifier.¹⁴ Concerning the reliability of the calculation of interaction energies in vacuum, a special consideration should be made. Molecular dynamics calculations have indicated a high mobility of polymer chains and a sufficiently wide free volume for a system such as a single KET molecule.¹⁴ For these reasons, the energies obtained in vacuum can be considered a good approximation of those referring to the solid phase.

An evaluation of the distances between the NH group of the KET molecule and CO of the amide was made as well. An increase in these distances was obtained moving from adduct 1 to adduct 3 in agreement with the decreasing interaction energies: −11.83, −11.52, and −6.00 kcal/mol, respectively (Figure 3a–c). Adduct 1 is the global minimum (Figure 3a), whereas the other geometries are local minima. The hydrogen-

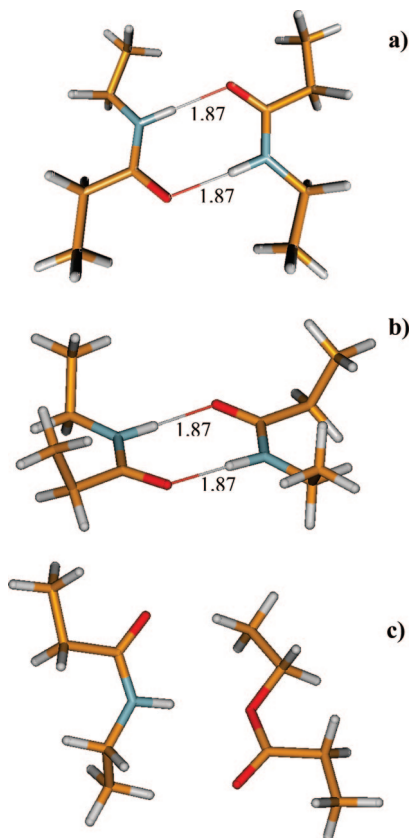


Figure 2. Minimum structures of (a,b) amide–amide and (c) ester–amide adducts evaluated at the B3LYP/6-31G* level of theory. (a) Adduct 1 is the global minimum, whereas (b) adduct 2 represents a local minimum. Hydrogen bonding has been selected according to the criterion based on internuclear distance.

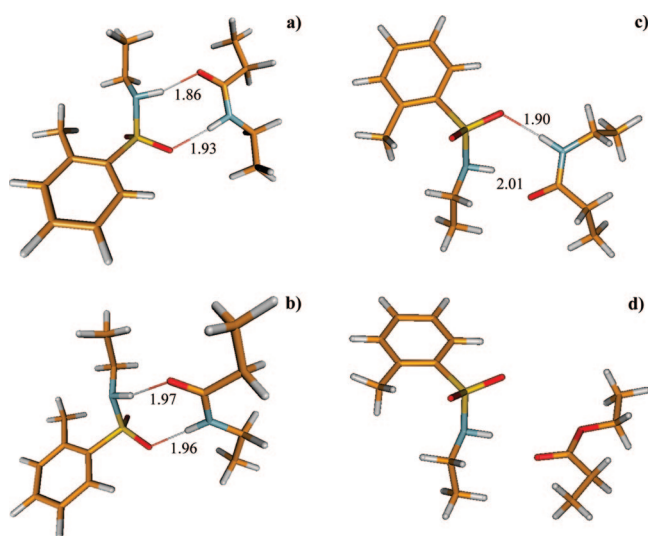


Figure 3. Minimum structures of (a–c) KET–amide and (d) KET–ester adducts evaluated at the B3LYP/6-31G* level of theory. (a) Adduct 1 is the global minimum, whereas adducts (b) 2 and (c) 3 are local minima. Hydrogen bonding has been selected according to the criterion based on internuclear distance.

bond lengths found in the global minimum are comparable to those calculated for the amide–amide adduct (Figure 2a). A local minimum was also identified for this adduct using the B3LYP/6-31G* level of theory (Figure 2b). The $\text{NH}\cdots\text{O}$ and $\text{NH}\cdots\text{O}=\text{C}$ distances for both the amide–ester and KET–ester complexes were also examined (Table 3). In this case, the distance between the NH of KET and the CO of the ester (Figure

TABLE 3: Bond Lengths (Å) for Ester–Amide and KET–Amide Systems Using Two Levels of Theory

system	B3LYP/6-31G*		X3LYP/6-311G**	
	$\text{N}-\text{H}\cdots\text{O}^-$	$\text{N}-\text{H}\cdots\text{O}=\text{C}$	$\text{N}-\text{H}\cdots\text{O}^-$	$\text{N}-\text{H}\cdots\text{O}=\text{C}$
amide–ester	2.18	2.80	2.19	2.81
KET–ester	3.12	2.03	3.13	2.06

TABLE 4: Infrared Frequencies (cm^{-1}) of $\text{C}=\text{O}$ Vibration for Ester, Ester–Amide, and KET–Ester Systems Using Two Levels of Theory

system	B3LYP/6-31G*	X3LYP/6-311G**
ester	1844.5	1827.4
ester–amide	1825.6	1808.0
KET–ester	1660.6, 1627.0	1616.0

3d) is smaller than the corresponding distance between the NH of the amide and the same carbonyl oxygen of the ester (Figure 2c). This finding is in agreement with the interaction energies evaluated both in solvent and in vacuum.

The values reported in Tables 1–3 support the interpretation that KET at low concentration would partially destroy the links between the polar functional groups (amide and ester) of the polymer. As a consequence, this produces the increase in the availability of the polar moieties and, thereby, in the hydrophilicity of the membranes. The theoretical values suitably match all of the experimental results.¹⁴

Additionally, the infrared frequencies associated with the normal modes of the ester carbonyl and amide groups were examined and are summarized in Table 4. The theoretical methods do not successfully reproduce the absolute values of the experimental frequencies. The values obtained using both computational methods overestimate the experimental frequencies by as much as $\sim 150\text{ cm}^{-1}$. Nevertheless the calculations yield trends that are in agreement with the experimental evidence. Moving from the ester molecule to the KET–ester adduct, a shift of the vibration frequency to lower values was found, confirming the strongest interaction between the modifier and the ester functional group of the PEBAX.¹⁴ The frequency of the carbonyl in the ester–amide complex was found to be close to that of the pure ester. In contrast, no difference was detected for the vibration frequencies of the $\text{C}=\text{O}$ group involved in the amide–amide and KET–amide adducts: 1710.2 and 1737.9 cm^{-1} for the amide–amide system and 1717.1 cm^{-1} for the KET–amide system.¹⁴

On the basis of these findings, the following theoretical mechanism can be postulated



where the asterisk (*) denotes free functional groups on the polymer chains. It is worth noting that the proposed mechanism is in fair agreement with all of the experimental evidence.^{9,10,12,14}

In particular, at low concentration of KET, KET interacts with the amide and ester moieties of the polymer, producing free polar groups. This enhances the hydrophilicity of the membrane and simultaneously reduces the packing density of the polymer chains. However, an additional contribution derived from single free KET molecules should not be neglected. Rather, with increasing KET concentration, the modifier molecules bind with the released amide and ester functional groups. This leads to a decreased hydrophilicity of the matrix, as has been observed experimentally.^{4,9,10}

This hydrogen-bonding domino mechanism might be generalized for other types of small guest molecules dispersed in different polymeric media. In particular, the guest compounds could be residue molecules of solvent used for the fabrication of membranes and entrapped in the polymeric matrixes. Also, this mechanism could be a powerful tool for analyzing swelling and aging phenomena, when molecules come into contact with membranes during separation processes.

Conclusions

This computational study investigates the role of hydrogen bonding involved in adducts that regulate the process of sorption into modified polymeric membranes. Here, the domino effect produced by an amphiphilic modifier (KET) on the hydrophilicity of a polymer (PEBAX) was examined. The calculated interaction energies show that the guest–host energies are in competition with host–host energies. At low concentration of modifier, this competition determines the increase in the availability of polymer polar moieties. This phenomenon is the key for interpreting the increase in sorption of polar penetrates in membranes, as has been observed experimentally. At high modifier concentration, the saturation of the polar moieties causes a decrease in the membrane hydrophilicity, because the modifiers again bind with the free functional groups of polymer. This theoretical interpretation is in fair agreement with all available experimental data.

Acknowledgment. The authors are grateful to INSTMI/CINECA for the computational support.

Supporting Information Available: Cartesian coordinates of the structures and total electronic energies of most important stationary points occurring in this investigation. This material is available free of charge via the Internet at <http://pubs.acs.org>.

References and Notes

- Petersen, K.; Nielsen, P. V.; Bertelsen, G.; Lawther, M.; Olsen, M. B.; Nilsson, N. H.; Mortensen, G. *Trends Food Sci. Technol.* **1999**, *10*, 52.
- Corveleyn, S.; De Smedt, S.; Remon, J. P. *Int. J. Pharm.* **1997**, *159*, 57.
- Minghetti, P.; Cilurzo, F.; Liberti, V.; Montanari, L. *Int. J. Pharm.* **1997**, *15*, 165.
- Gugliuzza, A.; Clarizia, G.; Golemme, G.; Drioli, E. *Eur. Polym. J.* **2002**, *38*, 235.
- Elberaichi, A.; Daro, A.; David, C. *Eur. Polym. J.* **1999**, *35*, 1217.
- Gugliuzza, A.; Drioli, E. *Polymer* **2005**, *46* (23), 9994.
- Nagai, K.; Freeman, B. D.; Cannon, A.; Allcock, H. R. *J. Membr. Sci.* **2000**, *172*, 167.
- Tocci, E.; Gugliuzza, A.; De Lorenzo, L.; Macchione, M.; De Luca, G.; Drioli, E. *J. Membr. Sci.* **2008**, *323*, 316.
- Gugliuzza, A.; Drioli, E. *Eur. Polym. J.* **2004**, *40/10*, 2381.
- (a) Gugliuzza, A.; Fagiani, R.; Garavaglia, M. G.; Spisso, A.; Drioli, E. *J. Colloid Interface Sci.* **2006**, *303*, 388. (b) Gugliuzza, A.; Fagiani, R.; Garavaglia, M. G.; Spisso, A.; Drioli, E. *J. Colloid Interface Sci.* **2007**, *306*, 192–193 (corrigendum to *J. Colloid Interface Sci.* **2006**, *303*, 388–403).
- Javaid, A.; Krapchetov, D. A.; Ford, D. M. *J. Membr. Sci.* **2005**, *246*, 181.
- Gugliuzza, A.; Drioli, E. *Polymer* **2003**, *44/7*, 2149.
- Gugliuzza, A.; De Luca, G.; Tocci, E.; De Lorenzo, L.; Drioli, E. *Desalination* **2006**, *200*, 256.
- Gugliuzza, A.; De Luca, G.; Tocci, E.; De Lorenzo, L.; Drioli, E. *J. Phys. Chem B* **2007**, *111*, 8868.
- Straatsma, T. P.; Apra, E.; Windus, T. L.; Dupuis, M. E.; Bylaska, J.; de Jong, W.; Hirata, S.; Smith, D. M.; Hackler, A. M.; Pollack, T. L.; Harrison, R. J.; Nieplocha, J.; Tipparaju, V.; Krishnan, M.; Brown, E.; Cisneros, G.; Fann, G. I.; Fruchtl, H.; Garza, J.; Hirao, K.; Kendall, R.; Nichols, J. A.; Tsemekhman, K.; Valiev, M.; Wolinski, K.; Anchell, J.; Bernholdt, D.; Borowski, P.; Clark, T.; Clerc, D.; Dachsel, H.; Deegan, M.; Dyall, K.; Elwood, D.; Glendening, E.; Gutowski, M.; Hess, A.; Jaffe, J.; Johnson, B.; Ju, J.; Kobayashi, R.; Kutteh, R.; Lin, Z.; Littlefield, R.; Long, X.; Meng, B.; Nakajima, T.; Niu, S.; Rosing, M.; Sandrone, G.; Stave, M.; Taylor, H.; Thomas, G.; van Lenthe, J.; Wong, A.; Zhang, Z. *NWChem, A Computational Chemistry Package for Parallel Computers*, version 5.1; Pacific Northwest National Laboratory: Richland, WA, 2005.
- Becke, A. D. *J. Chem. Phys.* **1993**, *98*, 5648.
- Xu, X.; Zhang, Q.; Muller, R. P.; Goddard, W. A., III. *J. Chem. Phys.* **2005**, *122*, 014105.
- van der Wijst, T.; Fonseca Guerra, C.; Swart, M.; Bickelhaupt, F. M. *Chem. Phys. Lett.* **2006**, *426*, 415.
- Fonseca Guerra, C.; Bickelhaupt, F. M.; Snijders, J. G.; Baerends, E. J. *J. Am. Chem. Soc.* **2000**, *122*, 4117.
- Zhao, Y.; Truhlar, D. G. *J. Phys. Chem. A* **2005**, *109*, 5656.
- Braeken, L.; Ramaekers, R.; Zhang, Y.; Maes, G.; Van der Bruggen, B.; Vandecasteele, C. *J. Membr. Sci.* **2005**, *2*, 52, 195.
- De Luca, G.; Tocci, E.; Drioli, E. *J. Mol. Struct.* **2005**, *739*, 163.
- Leng, Y.; Krstic, P. S.; Wells, J. C.; Cummings, P. T.; Dean, D. J. *J. Chem. Phys.* **2005**, *122*, 244721.
- Grabowski, S. J.; Robinson, T. L.; Leszczynski, J. *Chem. Phys. Lett.* **2004**, *386*, 44.
- Grabowski, S. J.; Sokalski, W. A.; Leszczynski, J. *J. Phys. Chem. A* **2005**, *109*, 4331.
- Grabowski, S. J.; Sokalski, W. A. *J. Phys. Org. Chem.* **2005**, *18*, 779.
- Gora, W. R.; Grabowski, S. J.; Leszczynski, J. *J. Phys. Chem. A* **2005**, *109*, 6397.
- Bader, R. F. W.; MacDougall, P. J.; Lau, C. D. H. *J. Am. Chem. Soc.* **1984**, *106*, 1594.
- Bader, R. F. W. *Atoms in Molecules: A Quantum Theory*; Oxford University Press: Oxford, U.K., 1990.
- Bader, R. F. W. *Chem. Rev.* **1991**, *91*, 893.
- Biegler-König, F.; Nguyen-Dang, T. T.; Tal, Y.; Bader, R. F. W. *J. Phys. B* **1981**, *14*, 2739.
- Kitaura, K.; Morokuma, K. *Int. J. Quantum Chem.* **1976**, *10*, 325.
- Yu, W.; Lin, Z.; Huang, Z. *ChemPhysChem* **2006**, *7*, 828.
- De Luca, G.; Mineva, T.; Russo, N.; Sicilia, E.; Toscano, M. Continuum Dielectric Models for the Solvent and Density Functional Theory: The State of the Art. In *Recent Advances in Density Functional Methods. Part II*; Chong, D. P., Ed.; World Scientific Publishing Co. Pte. Ltd.: Singapore, 1997; Chapter 3.
- Tomasi, J.; Mennucci, B.; Cammi, R. *Chem. Rev.* **2005**, *105*, 2999.
- Allen, M. P.; Tildesley, D. J. *Computer Simulation of Liquids*; Oxford University Press: Oxford, U.K., 1987.
- Klamt, A.; Schuurmann, G. *J. Chem. Soc., Perkin Trans.* **1993**, *2*, 799.
- De Luca, G.; Sicilia, E.; Russo, N.; Mineva, T. *J. Am. Chem. Soc.* **2002**, *124* (7), 1494.
- Stefanovich, E. V.; Truong, T. N. *Chem. Phys. Lett.* **1995**, *244*, 65.
- Barone, V.; Cossi, M.; Tomasi, J. *J. Chem. Phys.* **1997**, *107*, 3210.
- Simon, S.; Duran, M.; Dannenberg, J. J. *J. Chem. Phys.* **1996**, *105*, 11024.